

---

# Log-Likelihood Ratio Minimizing Flows: Towards Robust and Quantifiable Neural Distribution Alignment

---

Ben Usman<sup>1,2</sup> Nick Dufour<sup>2</sup> Avneesh Sud<sup>2</sup> Kate Saenko<sup>1</sup>

## Abstract

Distribution alignment has many applications in deep learning, including domain adaptation and unsupervised image-to-image translation. Most prior work on unsupervised distribution alignment relies either on minimizing simple non-parametric statistical distances such as maximum mean discrepancy, or on adversarial alignment. However, the former fails to capture the structure of complex real-world distributions, while the latter is difficult to train and does not provide any universal convergence guarantees or automatic quantitative validation procedures. In this paper we propose a new distribution alignment method based on a log-likelihood ratio statistic and normalizing flows. We show that, under certain assumptions, this combination yields a deep neural likelihood-based minimization objective that attains a known lower bound upon convergence. We experimentally verify that minimizing the resulting objective results in domain alignment that preserves the local structure of input domains.

## 1. Introduction

The goal of unsupervised domain alignment is to find a transformation of one dataset that makes it similar to another dataset while preserving the structure of the original. The majority of modern approaches to domain alignment directly search for a transformation of the data that minimizes an empirical estimate of some statistical distance - a non-negative quantity that takes lower values as datasets become more similar. The variability of what “similar” means in this context, which transformations are allowed, and whether data points themselves or their feature representations are aligned, leads to a variety of domain alignment methods. Unfortunately, existing estimators of statistical distances either restrict the notion of similarity to enable closed form estimation (Sun & Saenko, 2016), or rely on adversarial (min-max) training (Tzeng et al., 2017) that makes it very

difficult to quantitatively reason about the performance of such methods. In particular, the value of the optimized adversarial objective conveys very little about the quality of the alignment, which makes it difficult to perform automatic model selection on a new dataset pair. On the other hand, Normalizing Flows (Rezende & Mohamed, 2015) are an emerging class of deep neural density models that do not rely on adversarial training. They model a given dataset as a random variable with a simple known distribution transformed by an unknown invertible transformation, often parameterized using a deep neural network. Recent work on normalizing flows made great strides in defining new rich parameterizations for these invertible transforms (Kingma & Dhariwal, 2018; Grathwohl et al., 2018), but focused almost exclusively on density estimation.

In this paper we present the **Log-likelihood Ratio Minimizing Flow (LRMF)** - a new non-adversarial approach for aligning datasets “with respect to” a given family of distributions  $\mathcal{M}$  (e.g. normal distributions, or PixelCNNs with fixed architecture, etc.). It uses unique properties of normalizing flows to turn an otherwise adversarial optimization problem into a minimization problem. More specifically, we consider two datasets  $A$  and  $B$  equivalent with respect to  $\mathcal{M}$  if there is a single density model in  $\mathcal{M}$  that is optimal for both  $A$  and  $B$ . If we fit a density model  $P_A$  to  $A$  and  $P_B$  to  $B$ , and then fit another “shared” model  $P_S$  to the combined dataset containing samples from both  $A$  and  $B$ , the average log-likelihood scores of the shared model  $P_S$  on  $A$  and  $B$  would match average log-likelihoods of  $P_A$  on  $A$  and  $P_B$  on  $B$  only if  $P_S$  was an optimal density model for both  $A$  and  $B$  independently, i.e. these datasets are equivalent w.r.t.  $\mathcal{M}$ . We want to find a transformation  $T(x)$  that transforms dataset  $A$  in a way that makes  $A' \triangleq T(A)$  equivalent to  $B$ . We do that by minimizing the gap between log-likelihood scores of the “shared” model  $P_S$  and “private” models  $P_A$  and  $P_B$ . For general  $\mathcal{M}$ , such  $T(x)$  can be found only by solving a min-max optimization problem, but in this paper we show that if  $T(x, \phi)$  is a family of normalizing flows, then the flow  $T(x, \phi^*)$  that makes  $T(A, \phi^*)$  and  $B$  equivalent with respect to  $\mathcal{M}$  can be found by minimizing a single objective that attains zero upon convergence. This enables automatic model validation and hyperparameter tuning on the held out set.

---

Boston University<sup>1</sup>, Google AI<sup>2</sup>.

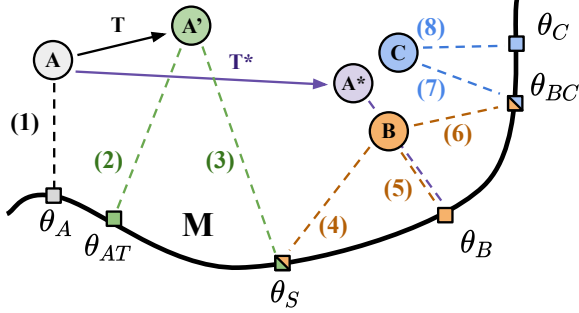


Figure 1. In the space of probability distributions over  $\mathcal{X} \subset \mathbb{R}^n$ , empirical distributions of datasets  $A$  and  $B$  can be thought of as points, and the parametric density family  $\mathcal{M}(\theta)$  as a surface. We want to find a transformation  $T(x)$  that makes  $A' \triangleq T(A)$  and  $B$  “equivalent” with respect to  $\mathcal{M}$ . More specifically, we want the optimal density estimator  $\theta_{AT}$  for the transformed dataset  $A'$  to be optimal for  $B$  as well, like it is for  $A^*$  and  $B$ . In this paper, we show that if  $T(x)$  is a family of normalizing flows, then, for an arbitrary family of densities  $\mathcal{M}(\theta)$ , the optimal  $T^*$  that makes  $T^*(A)$  and  $B$  share a projection onto  $\mathcal{M}$  can be found by solving a simple non-adversarial minimization problem (Eq 2). The majority of prior work on aligning datasets with respect to a given family of discriminating functions either severely restricts that family, or relies on adversarial training. Our objective works with arbitrary density models as “discriminators” and provides a single minimization objective with known lower bound.

To sum up, the novel non-adversarial data alignment method presented in this paper combines the clear convergence criteria found in non-parametric and simple parametric approaches and the power of deep neural discriminators used in adversarial models. Our method finds a transformation of one dataset that makes it “equivalent” to another dataset with respect to the specified family of density models. We show that if that transformation is restricted to a normalizing flow, the resulting problem can be solved by minimizing a single simple objective, and that this objective attains zero only if two domains are correctly aligned. We experimentally verify this claim, and show that the proposed method preserves local structure of the transformed distribution, and that it is robust to both model misspecification by both over- and under-parameterization.

## 2. Log-Likelihood Ratio Minimizing Flow

In this section, we formally define the proposed method for aligning distributions. We assume that  $\mathcal{M}(\theta)$  is a manifold of densities, and we project datasets onto  $\mathcal{M}$  by maximizing the likelihood of these datasets across models from  $\mathcal{M}$ , or equivalently by minimizing the KL divergence with corresponding empirical Dirac delta mixture “densities”. We introduce the log-likelihood ratio pseudo-distance and show its relation to the test statistic of the same name. Intuitively, if we project datasets  $A$  and  $B$  onto  $\mathcal{M}$  independently ( $\theta_A$

and  $\theta_B$ ), and also find a point  $\theta_S$  on  $\mathcal{M}$  that minimizes the combined distance from  $A$  and  $B$  to that  $\theta_S$ , then the log-likelihood ratio distance would equal the difference between the approximation quality (negative log-likelihood) of that optimal “shared” approximation and the two optimal “private” approximations (Definition 2.1). Figure 1 illustrates how this quantity changes as two datasets become more similar: the log-likelihood ratio distance between  $A'$  and  $B$  [(3)+(4)-(2)-(5)] is larger than the log-likelihood ratio distance between  $B$  and  $C$  [(6)+(7)-(8)-(5)] because the shared approximation  $\theta_{BC}$  for  $B$  and  $C$  approximates them almost as well as their private approximations  $\theta_B$  and  $\theta_C$ . After defining the distance we consider the problem of finding a transformation that would minimize this distance (Eq 1) and provide an intuition on how different components of the objective would affect the learned transformation if we minimized it directly (Figure 2). In general, finding such a transformation would require solving an adversarial optimization problem, but we show that if the transformation is restricted to the family of normalizing flows, then the optimal one can be found by minimizing a simple non-adversarial objective (Theorem 2.3). We illustrate this result with an example that can be solved analytically: we show that minimizing the log-likelihood ratio distance between two random variables with respect to the normal density family is equivalent to directly matching their first two moments.

First, let specify the parametric family of distributions  $\mathcal{M}(\theta)$  we are going to align our datasets “against”. We assume that the negative log-likelihoods of distributions in  $\mathcal{M}$  over some fixed domain  $\mathcal{X} \subset \mathbb{R}^n$  is given by

$$L(X, \theta) = -\log P_M(X|\theta)$$

**Definition 2.1.** Let us define the **log-likelihood ratio distance**  $d_\Lambda(A, B; \mathcal{M})$  between datasets  $A$  and  $B$  from  $\mathcal{X}$  with respect to the family of densities  $\mathcal{M}$  as the difference between negative log-likelihoods  $L(X, \theta)$  of optimal models with “shared” and “private” parameters  $\theta$ :

$$\begin{aligned} d_\Lambda(A, B; \mathcal{M}) &= \min_{\theta_S} \left[ L(A, \theta_S) + L(B, \theta_S) \right] \\ &\quad - \min_{\theta_A} L(A, \theta_A) - \min_{\theta_B} L(B, \theta_B) \\ &= \min_{\theta_S} \max_{\theta_A, \theta_B} \left[ L(A, \theta_S) + L(B, \theta_S) \right. \\ &\quad \left. - L(A, \theta_A) - L(B, \theta_B) \right] \end{aligned}$$

The expression above is also the log-likelihood ratio test statistic  $\log \Lambda_n$  for the null hypothesis  $H_0 : \theta_A = \theta_B$  for the model described by the log-likelihood function:

$$\log P(A, B | \theta_A, \theta_B) = \log P_M(A, \theta_A) + \log P_M(B, \theta_B).$$

**Lemma 2.1.** The log-likelihood ratio distance is always non-negative

$$d_\Lambda(A, B; \mathcal{M}) \geq 0$$

and equals zero only if there exists a single “shared” model  $\theta_S$  that approximates both  $A$  and  $B$  as well as their “private” optimal approximations:

$$\begin{aligned} d_\Lambda(A, B; \mathcal{M}) &= 0 \Leftrightarrow \\ \exists \theta_S \forall X \in \{A, B\} \quad L(X, \theta_S) &= \min_\theta L(X, \theta). \end{aligned}$$

*Proof.* If we define  $f(x) = L(A, x)$  and  $g(x) = L(B, x)$ , the first statement  $d_\Lambda \geq 0$  follows from the fact that

$$\begin{aligned} \forall x \quad f(x) + g(x) &\geq \min_x f(x) + \min_x g(x) \Rightarrow \\ \min_x (f(x) + g(x)) - \min_x f(x) - \min_x g(x) &\geq 0 \end{aligned}$$

and second statement  $f(x^*) = \min_x f(x)$  comes from the fact that the equality holds only if there exists such  $x^*$  that

$$f(x^*) + g(x^*) = \min_x f(x) + \min_x g(x)$$

since for all other  $x$  holds  $f(x) \geq \min_x f(x)$  and analogously  $g(x^*) = \min_x g(x)$  since  $g(x) \geq \min_x g(x)$ .  $\square$

Now we will introduce the parametric family of transformations  $T(x, \phi)$  and will show that the adversarial problem that arises if we try to find  $\phi$  that minimizes the log-likelihood ratio distance  $\min_\phi d_\Lambda(T(A, \phi), B)$ , i.e.

$$\min_\phi \min_{\theta_S} \max_{\theta_{AT}, \theta_B} \left[ L(T(A, \phi), \theta_S) + L(B, \theta_S) - L(T(A, \phi), \theta_{AT}) - L(B, \theta_B) \right] \quad (1)$$

can be solved using non-adversarial minimization if  $T(x, \phi)$  is a parametric family of flows. But first, let us examine the intuition on how different components of the objective above would have effected the transformed dataset if we optimized them directly. The model  $\theta_{AT}$  in the definition above stands for the optimal approximation of  $T(A, \phi)$ . Figure 2 shows that, when minimized over  $\phi$ , the first component of the loss, namely  $L(T(A, \phi), \theta_S)$ , pulls the transformed dataset  $A'$  towards the best shared model  $\theta_S$  and the third component  $-L(T(A, \phi), \theta_{AT})$  pushes it away from its optimal approximation on  $\mathcal{M}$ , therefore ensuring that  $A'$  becomes more similar to  $B$  with respect to  $\mathcal{M}$  without collapsing onto  $\mathcal{M}$ . For example, if two datasets were already equivalent w.r.t.  $\mathcal{M}$ , but not necessarily on  $\mathcal{M}$  itself, the objective above would *not* encourage them to move towards  $\mathcal{M}$ . When optimized over  $\theta_S$  and  $\theta_{AT}$ , first three components of the objective above ensure that  $\theta_{AT}$  is still an optimal approximation of  $A'$  and  $\theta_S$  is still an optimal approximations of  $A'$  and  $B$  combined. The last component of the loss optimized over  $\theta_B$  is a constant that can be computed separately.

The optimization problem stated above is still adversarial, but the lemma presented below enables us to find the optimal transformation by simply minimizing a modified version of the objective (1) using an iterative method of one’s choice.

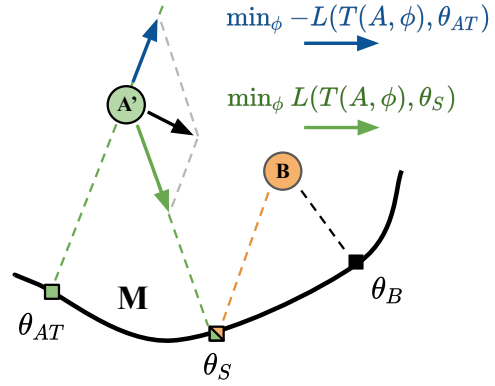


Figure 2. Optimizing the log-likelihood ratio distance (Eq 1) between the transformed dataset  $A'$  and the target dataset  $B$  with respect to the transformation parameter  $\phi$  results in the dataset being pulled towards the shared model  $\theta_S$  (green) and away from the best approximating model  $\theta_{AT}$  (blue), resulting in the total combined gradient (black) that points towards the target dataset  $B$ .

**Lemma 2.2.** *If  $\mathcal{M}$  can approximate  $A \sim P_A$  well, i.e.*

$$\min_\theta L(A, \theta) = -\log P_A(A)$$

where  $P_A$  is the true data distribution of  $A$ , and if  $T(x; \phi)$  is the family of normalizing flows from  $\mathcal{X}$  to itself, then the amount of additional entropy (negative log-likelihood) the transformation  $T(x, \phi)$  induces upon  $A$  according to  $\mathcal{M}$  is bounded by the actual amount of entropy it induces upon it:

$$\begin{aligned} \min_{\theta_{AT}} L(T(A, \phi), \theta_{AT}) - \min_{\theta_A} L(A, \theta_A) \\ \geq -\log \det |\nabla_x T_\phi^{-1}(T_\phi(A))|. \end{aligned}$$

*Proof.* We know from the change of variable formula that if  $T_\phi$  is a normalizing flow and  $X = T_\phi(Z)$  where  $Z \sim P_Z$ , then the log-likelihood can be expressed as

$$\log P_T^Z(X|\phi) = \log P_Z(T_\phi^{-1}(X)) + \log \det |\nabla_x T_\phi^{-1}(X)|.$$

Following the same logic, if  $A' = T_\phi(A)$  and  $A \sim P_A$ , and considering the invertibility of  $T_\phi$ , we can express the true distribution of  $A'$  as follows (the superscript in  $P_T^A$  indicates that we used  $P_A$  instead of  $P_Z$  in that flow likelihood):

$$\begin{aligned} \log P_T^A(A'|\phi) &= \log P_A(T_\phi^{-1}(T_\phi(A))) + \log \det |\nabla_x T_\phi^{-1}(T_\phi(A))| \\ &= \log P_A(A) + \log \det |\nabla_x T_\phi^{-1}(T_\phi(A))| \end{aligned}$$

Considering that  $\mathcal{M}$  can approximate  $A$  well, i.e.  $-\min_\theta L(A, \theta) = \log P_A(A)$ , but might not approximate the true distribution of the transformed dataset  $P_T^A$  as well:

$$\begin{aligned} -\min_\theta L(A', \theta) \leq \log P_T^A(A'|\phi) \Rightarrow \\ -\min_\theta L(A', \theta) \leq -\min_\theta L(A, \theta) + \log \det |\nabla_x T_\phi^{-1}(T_\phi(A))| \end{aligned}$$

after multiplying both sides by negative one and reordering the terms we get the statement of the lemma.  $\square$

We get a simpler formula that directly specifies which models should be trained on what data (and is therefore easier to translate to code), if we express the average logarithm of the determinant of the Jacobian (of the inverse transform computed at the transformed dataset) using the log-likelihood of the corresponding flow  $\log P_T$  with an arbitrarily choice of prior  $P_Z$ , because it is canceled out:

$$\log \det |\nabla_x T_\phi^{-1}(T_\phi(A))| = \log P_T(T(A, \phi), \phi) - \log P_Z(A).$$

**Definition 2.2.** Let us define the **log-likelihood ratio minimizing flow (LRMF)** for a pair of datasets  $A$  and  $B$  on  $\mathcal{X}$ , the family of densities  $\mathcal{M}(\theta)$  on  $\mathcal{X}$  with the negative log-likelihood  $L(X, \theta)$ , and the parametric family of normalizing flows  $T(x; \phi)$  from  $\mathcal{X}$  onto itself with likelihood  $P_T(x, \phi)$  and an arbitrary choice of prior  $P_Z(x)$ , as the flow  $T(x; \phi^*)$  that minimizes the following objective

$$\min_{\phi} \min_{\theta_S} [L(T(A, \phi), \theta_S) + L(B, \theta_S) + \log P_T(T(A, \phi), \phi) - c(A, B)]. \quad (2)$$

where the constant

$$c(A, B) = \log P_Z(A) + \min_{\theta_A} L(A, \theta_A) + \min_{\theta_B} L(B, \theta_B)$$

does not depend on  $\theta_S$  and  $\phi$ , and can be precomputed in advance.

**Theorem 2.3.** If the LRMF minimization objective (Eq 2) attains value  $V$  at the optimum, then the adversarial log-likelihood ratio distance (Eq 1) between the transformed source and target datasets can be bounded as

$$0 \leq d_\Lambda(T(A, \phi^*), B; \mathcal{M}) \leq V.$$

This theorem follows from the definition of  $d_\Lambda$  and two lemmas provided above. This result enables us to find the parameters of the normalizing flow  $\phi$  that make  $T(A, \phi)$  and  $B$  equivalent with respect to  $\mathcal{M}$  using existing gradient decent iterations with known convergence guarantees. Intuitively, the reason why we were able to replace the adversarial problem (1) with a minimization problem (2) is that the third term in Eq 1 acts as an entropy-based “discriminator”, but the flow family provides a closed-form expression for estimating the extra entropy the transformation induces upon the dataset without solving an optimization problem.

The example below shows that the affine transform that minimizes the log-likelihood ratio distance between two random variables with respect to normal density family  $\mathcal{M}$  corresponds to shifting and scaling one variable to match two first moments of the other, which makes intuitive sense.

**Example 2.1.** Let us consider two random variables  $A, B$  with moments  $\mu_A, \mu_B, \sigma_A^2, \sigma_B^2$ , restrict  $\mathcal{M}$  to normal densities, and the transform  $T(x; \phi)$  to the affine family:  $T(x; a, b) = ax + b$ . The negative log-likelihood of the

normal distribution depends on its variance as follows:

$$\min_{\mu, \sigma} \mathbb{E}_X L(X; \mu, \sigma) = \frac{1}{2} \log(2\pi e \sigma_X^2) = \log \sigma_X + C$$

In our case

$$c(A, B) = \mathbb{E} \log P_Z(B) + \log \sigma_A + \log \sigma_B + 2C$$

$$\log P_T(X; a, b) = -\log a + \mathbb{E} \log P_Z\left[\frac{X-b}{a}\right]$$

$$\log P_T(T(A; a, b); a, b) = -\log a + \mathbb{E} \log P_Z(A)$$

Using the fact that the variance of the equal mixture can be expressed using moments of its components, we can solve optimization over  $\theta_S = (\mu_S, \sigma_S)$  analytically

$$\begin{aligned} \sigma_{XY}^2 &= \frac{1}{2}(\sigma_X^2 + \sigma_Y^2) - \frac{1}{4}(\mu_X - \mu_Y)^2 \\ \min_{\mu_S, \sigma_S} [L(T(A; a, b); \mu_S, \sigma_S) + L(B; \mu_S, \sigma_S)] &= \\ &= \log\left(\frac{1}{2}(a^2\sigma_A^2 + \sigma_B^2) - \frac{1}{4}(\mu_A + b - \mu_B)^2\right) + 2C. \end{aligned}$$

Combining expressions above gives us the final objective:

$$\begin{aligned} d_\Lambda(T(A, a, b), B, \mathcal{M}) &= -\log \sigma_A - \log \sigma_B - \log a + \\ &+ \log\left(\frac{1}{2}(a^2\sigma_A^2 + \sigma_B^2) - \frac{1}{4}(\mu_A + b - \mu_B)^2\right) \end{aligned}$$

which can be solved analytically by setting the derivatives of  $d_\Lambda$  wrt  $a$  and  $b$  to zero and gives:

$$a^* = \frac{\sigma_B}{\sigma_A}, \quad b^* = \mu_B - \mu_A.$$

**On replacing the Gaussian prior with a learned density in normalizing flows.** We explored whether a similar distribution alignment effect can be achieved by directly fitting a density model to the target distribution  $B$  to obtain the optimal  $\theta_B$  first, and then fitting a flow model  $T(x, \phi)$  to the dataset  $A$  but replacing the Gaussian prior with the learned density of  $B$ , essentially training the flow to map  $A$  to  $P_M(x, \theta_B)$  instead of usual  $A$  to  $P_Z(x)$

$$\begin{aligned} \min_{\phi} [ &\log P_T(A, \phi) - \log P_Z(T^{-1}(A, \phi)) \\ &+ \log P_M(T^{-1}(A, \phi) | \theta_B)]. \end{aligned}$$

While this procedure worked on distributions that were very similar to begin with, in the majority of cases the log-likelihood fit to  $B$  did not provide informative gradients when evaluated on the transformed dataset, as the KL-divergence between distributions with disjoint supports is infinite  $L(T^{-1}(A, \phi), \theta_B) = \infty$ . Moreover, even when this objective did not explode, multi-modality of  $P_M(x, \theta_B)$  often caused the learned transformation to map  $A$  to one of its modes. Training both  $\phi$  and  $\theta_B$  jointly or in alternation yielded a procedure that was very sensitive to the choice of learning rates and hyperparameters, and failed silently, which were the reasons we abandoned adversarial methods in the first place. The LRMF method described



in this paper is not susceptible to this problem, because we never train a density estimator on one dataset and evaluate its log-likelihood on another dataset. The LRMF objective (2) shows that we both train and evaluate  $\theta_S$  on  $T(A, \phi)$  and  $B$ , and train and evaluate  $\log P_T(x, \phi)$  on  $T(A, \phi)$ .

#### On directly estimating likelihood scores across domains.

One could suggest to estimate the similarity between datasets by directly evaluating and optimizing some combination of  $L(A, \theta_B)$  and  $L(B, \theta_A)$ . Unfortunately, high likelihood values themselves are not very indicative of belonging to the dataset used for training the model, especially in higher dimensions, as explored by Nalisnick et al. (2018). One intuitive example of this effect in action is that for a high-dimensional normally distributed  $x \sim \mathcal{N}_d(0, I)$  the probability of observing a sample in the neighbourhood of zero  $P(\|x\| \leq r)$  is small, but if we had a dataset  $\{y_i\}_{i=0}^n$  sampled from that neighbourhood  $\|y_i\| \leq r$ , its log-likelihood  $\sum_i \log \mathcal{N}_d(y_i | 0, I)$  would be high, even higher than the likelihood of the dataset sampled from  $\mathcal{N}_d(0, I)$  itself. The proposed method, however, is not susceptible to this issue as we always evaluate the likelihood on the same dataset we used for training.

**On using the score test instead of the likelihood ratio.** If we perform the Taylor expansion of the log-likelihood ratio statistic near the optimal shared model  $\theta_S$ , we get the score test statistic - a “lighter” version of the log-likelihood ratio test that requires training only a single model. Intuitively, if we train a model from  $\mathcal{M}$  simultaneously on two datasets  $A$  and  $B$  until convergence, i.e. until the average gradient of the loss w.r.t. weights  $g_X = \nabla_{\theta} L(X, \theta)$  summed across both datasets becomes small  $\|g_A + g_B\| \leq \varepsilon$ , then the combined norm of two gradients computed across each dataset independently would be small  $\|g_A\| + \|g_B\| \leq \varepsilon$ , only under the null hypothesis ( $A$  and  $B$  are equivalent w.r.t.  $\mathcal{M}$ ). From our experience, this approach works well for detecting the presence of the domain shift, but is hardly suitable for direct minimization. We also would like to point readers to the relation between such score-based objective and the recently proposed Invariant Risk Minimization objective (Arjovsky et al., 2019), discussed in more detail in the supplementary.

**On matching the parameters of density models.** Two major objections we have to directly minimizing the distance between parameters  $\theta$  of density models fitted to respective datasets  $\|\theta_{AT} - \theta_B\|$  are that: a) the set of parameters that describes a given distribution might be not unique, and this objective does not consider this case; and b) one would have to employ some higher-order derivatives of the likelihood function to account for the fact that not all parameters contribute equally to the learned density function, therefore rendering this objective computationally infeasible to optimize for even moderately complicated density models.

### 3. Related work

**Domain Adaptation.** Early neural feature-level domain adaptation methods such as DAN (Long et al., 2015) or JAN (Long et al., 2017) directly optimized closed form estimates of non-parametric statistical distances (e.g. maximum mean discrepancy, earth mover’s distance or energy distance) between deep features of data points from two domains. Other early neural DA methods such as DeepCORAL (Sun & Saenko, 2016) approximated domain distributions via simple parametric density models with known closed form expressions for the KL-divergence, e.g. pairs of Gaussians. Unfortunately, both non-parametric and simple parametric models are limited to feature-level adaptation because of their inability to capture the internal structure of complicated real-world datasets. These limitations were addressed by recent adversarial (GAN-based) parametric approaches that used deep convolutional networks for domain discrimination, including DANN (Ganin et al., 2016) and ADDA (Tzeng et al., 2017). Unfortunately, the adversarial nature of these objectives makes respective models notoriously hard to train and provides no domain-agnostic convergence validation and automated model selection protocols beyond visually assessing generated images, or by evaluating the performance on a different downstream task, if ground truth target labels are available.

**Normalizing Flows.** The main assumption behind normalizing flows (Rezende & Mohamed, 2015) is that the observed data can be modeled as a simple distribution transformed by an unknown invertible transformation. Then the density at a given point can be estimated using the change of variable formula by estimating the determinant of the Jacobian of that transformation at the given point. The main challenge in developing such models is to define a class of transformations that are invertible, rich enough to model real-world distributions, and simple enough to enable direct estimation of the aforementioned Jacobian determinant. Most notable examples of recently proposed normalizing flows include Real NVP (Dinh et al., 2016), as the first to fit a good flow model of a real-world dataset, GLOW (Kingma & Dhariwal, 2018) built upon Real NVP (more general learnable permutations at multiple scales) and the first to show that a large enough flow can model high resolution images, and the recent FFJORD (Grathwohl et al., 2018), that made use of the fact that the forward simulation of an ordinary differential equation with an arbitrary velocity field satisfies all the requirements for a practically useful normalizing flow.

**Composition of inverted flows.** One natural alternative to the approach proposed in this paper, explored by the authors of the AlignFlow (Grover et al., 2019), is to train two flow models  $F$  and  $G$  on datasets  $A$  and  $B$  and to use the “back-to-back” composition  $F \circ G^{-1}$  to map points from  $A$  to

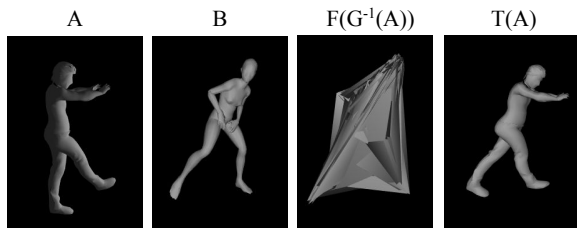


Figure 3. If we train two normalizing flows:  $G$  on vertices of the mesh  $A$  and  $F$  on  $B$ , the vertex distribution of  $F(G^{-1}(A))$  matches  $B$ , but the local structure of the original manifold is completely distorted. On the other hand, training a separate flow  $T$  to match  $T(A)$  with  $B$  using the likelihood objective does not erase the local structure.

$B$ . We argue that the structure of the dataset manifold is completely erased since each flow is independently trained to map the structured input to the structureless standard Gaussian. Figure 3 shows what happens if we treat vertices of two meshes as observations from two mesh surface point distributions, fit two different flows, and pass one vertex cloud through the back-to-back composition of learned flows. The number of points in each sub-volume of  $B$  matches the corresponding number in the transformed point cloud (third column)  $F(G^{-1}(A))$ , but if we draw the faces of the original mesh  $A$  at new vertex position, we observe that all relations between vertices (the local structure of the original mesh surface manifold) is distorted beyond recognition. We argue that this must be due to the fact that each flow is trained to “fold” a two-dimensional surface distribution into the interior of the three-dimensional Gaussian ball independently, and two “incompatible foldings” render correspondences between  $F^{-1}(B)$  and  $G^{-1}(A)$  meaningless. Authors of the AlignFlow suggest to share weights between  $F$  and  $G$  to mitigate this issue, but we believe that this only a partial solution that does not addresses the core of the issue. Training a flow model to directly map one distribution to the other with a likelihood objective (forth column) preserves the local structure of the original distribution. Authors of the PointFlow (Yang et al., 2019) showed that a hierarchical FFJORD trained on point clouds of mesh surfaces can be used to align these point clouds in the  $F \circ G^{-1}$  fashion. But the point correspondences found by the PointFlow are again due to the spatial co-occurrence of respective parts of meshes (left bottom leg of the humanoid is always at the bottom left) and do not respect the structure of respective surface manifolds.

**CycleGAN with normalizing flows.** RevGAN (van der Ouderaa & Worrall, 2019) made use of GLOW (Kingma & Dhariwal, 2018) to enforce the cycle consistency of the CycleGAN on the architecture level, but left the loss and the adversarial training procedure unchanged. We believe that the normalizing flow model for dataset alignment should make use of the maximum likelihood principle since the ability to fit rich models with plain minimization and validate

their performance on held out sets are the primary selling points of normalizing flows that should not be dismissed.

**Likelihood ratio testing for out-of-distribution detection.** Nalisnick et al. (2018) recently observed that likelihood scores themselves are not sufficient for determining whether a given data point came from the same dataset as the one used for training the density model. Independently from us, a recent paper by Ren et al. (2019) suggested to use log-likelihood ratio test for out-of-distribution detection of genomic sequences. We go one step further and propose a simple procedure for minimizing this measure of the dataset discrepancy.

## 4. Results

In this section we show experiments on simple datasets that verify that minimizing the proposed LRMF objective (Eq 2) with Gaussian, RealNVP and FFJORD density estimators and transformations does indeed result in dataset alignment. We also show that both under- and over-parameterized LRMFs performed well in practice, and that resulting flows preserved local structure of aligned datasets. We also show that the RealNVP LRMF produced a semantically meaningful alignment in the embedding space of an autoencoder trained simultaneously on two digit domains (MNIST and USPS). We provide LaTeXed pseudo-code of the training algorithm and jupyter notebooks with code in JAX (Bradbury et al., 2018) and TensorFlow Probability (Dillon et al., 2017) to reproduce these experiments in the supplementary.

**Data.** The *blobs* dataset pair contains two samples of size  $N = 100$  from two 2-dimensional Gaussians. The moons dataset contains two pairs of moons rotated  $50^\circ$  relative to one another. The exact parameters are given in the supplementary. Experiments on MNIST and USPS were conducted in the 32-dimensional embedding space of a VAE-GAN trained on unlabeled images from both digit domains scaled to  $28 \times 28$ .

**Affine LRMF w.r.t. the Gaussian family.** We parameterized the positive-definite transformation as  $T(x, A, b) = A^T A \cdot x + b$  and the Gaussian density with parameters  $(\mu, \Sigma^{-\frac{1}{2}})$  to ensure that  $\Sigma$  is always positive definite. The first line in Figure 4 shows that, just like in the Example 2.1, the affine likelihood ratio minimizing flow with respect to the normal density family matches first two moments of aligned distributions. Blue, red and cyan points represent  $A$ ,  $B$  and  $T(A)$  respectively and ellipses represent  $3\sigma$  levels of  $\theta_{AT}$ ,  $\theta_B$  and  $\theta_S$ . The loss converges to zero, and  $P_M(x, \theta_S)$  equals  $P_M(x, \theta_B)$  at the optima. The second row contains an experiment on the *moons* dataset pair containing two pairs of moons (blue and red). As in the previous experiment, the affine LRMF w.r.t. the normal density matches first two moments of aligned distributions. The

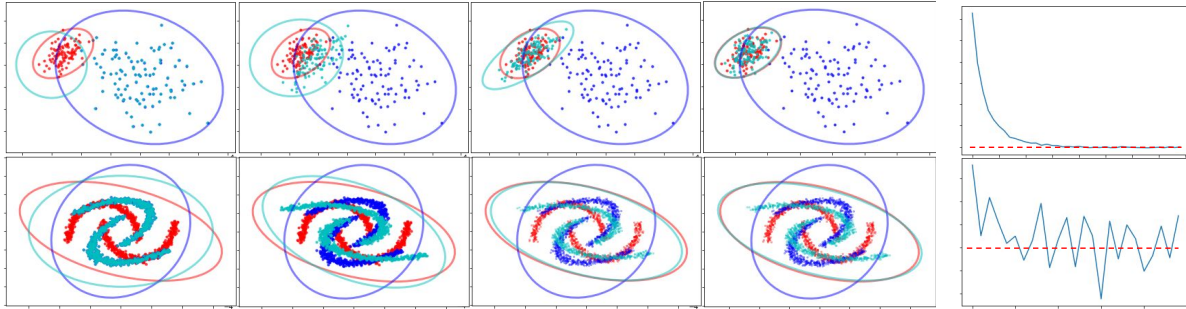


Figure 4. The dynamics of training an affine log-likelihood ratio minimizing flow (LRMF) w.r.t. the Gaussian family on the blob and moons datasets. The LRMF is trained to match  $A$  (blue) with  $B$  (red), its outputs  $T(A)$  are colored with cyan, circles indicate  $3\sigma$  levels of  $\theta_A$ ,  $\theta_B$  and  $\theta_{AT}$  respectively. This experiment shows that even a severely *under-parameterized LRMF* does a good job at aligning distributions (second row). As in **Example 2.1**, the optimal affine LRMF w.r.t. Gaussian family matches first two moments of given datasets. Rightmost column shows LRMF convergence.

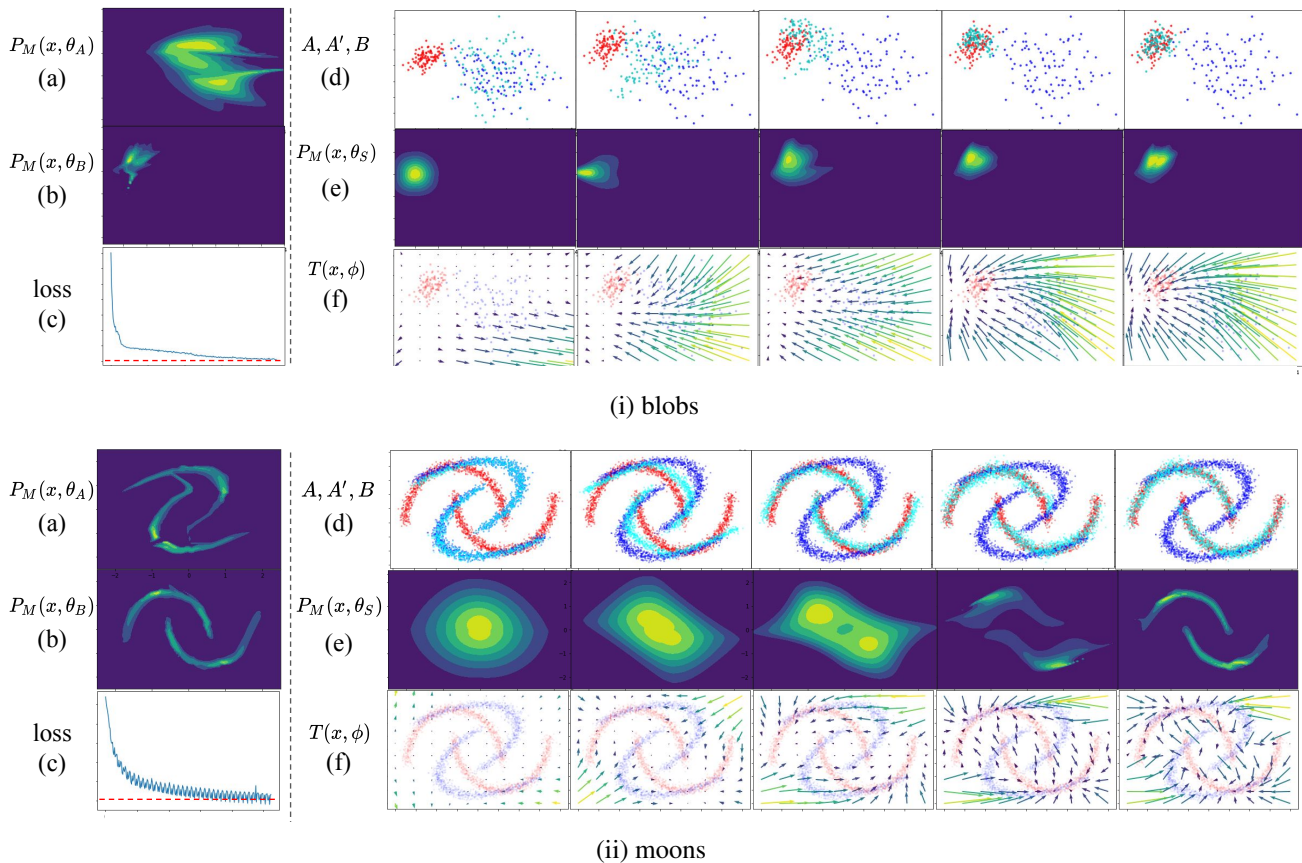


Figure 5. The dynamics of training a Real NVP log-likelihood ratio minimizing flow (LRMF) on the blob and moons datasets. This experiment shows that even a severely *overparameterized LRMF* does a good job at aligning distributions: RealNVP clearly overfits to the blob dataset but learns a good alignment nevertheless. **(a, b)** The Real NVP density estimators fitted to datasets  $A$  (blue) and  $B$  (red). **(c)** The LRMF objective (Eq 2) decreases over time and reaches zero when two datasets are aligned. The red line indicates the zero loss level. **(d)** The evolution  $A$  (blue),  $A' = T(A, \phi)$  (cyan) and  $B$  (red). **(e)** The probability density function of the shared model  $P_M(x, \theta_S)$  fitted to  $A'$  and  $B$ . When LRMF objective converges,  $P_M(x, \theta_S)$  matches  $P_M(x, \theta_B)$ . **(f)** The visualization of the trained normalizing flow  $T$ , at each point  $x$  we draw a vector pointing along the direction  $v = x - T(x, \phi)$  with color intensity and length proportional to  $v$ .



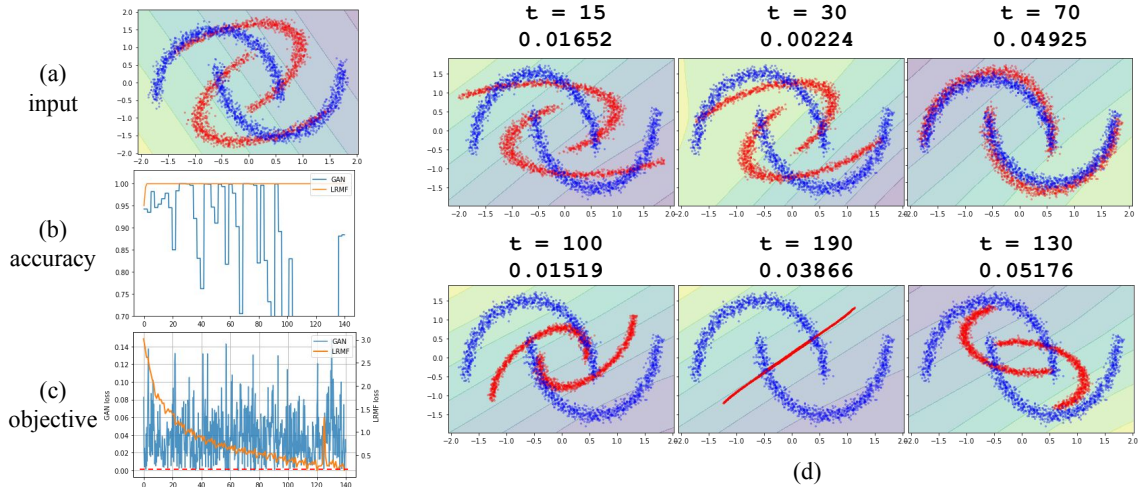


Figure 6. The dynamics of training a GAN with Spectral Normalization (SN-GAN) on the moons dataset. The adversarial framework provides means for aligning distributions against rich families of parametric discriminators, but requires the right choice of learning rate and an external early stopping criterion, because the absolute value of the adversarial objective (c, d) is not indicative of the actual alignment quality (b) even in low dimensions. The proposed LRMF method has a clear minimization objective with known lower bound.

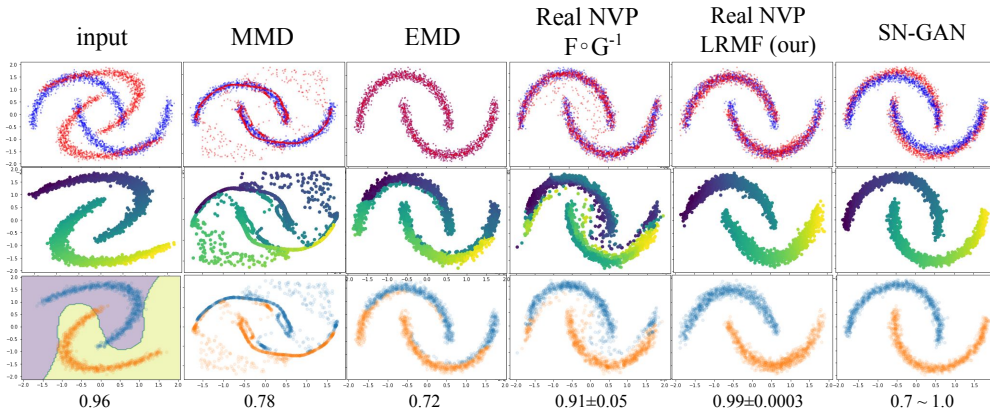


Figure 7. Among the non-adversarial alignment objectives, only LRMF preserves the local structure of the transformed manifold. The top row shows how well two domains (red and blue) are aligned by different methods trained to transform the red dataset to match the blue dataset. The middle row shows new positions of points colored consistently with the first column. Each domain contains two moons and the bottom row shows what happens to each moon from the red dataset after the alignment. Numbers at the bottom of each figure show the accuracy of the 1-nearest neighbor classifier trained on labels from the blue domain and evaluated on transformed samples from the red domain. The dynamics of the LRMF alignment can be found in Figure 5.

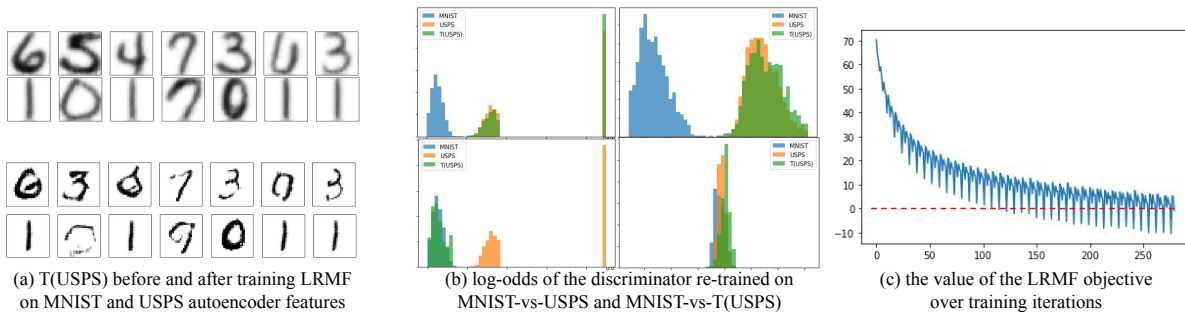


Figure 8. RealNVP LRMF successfully semantically aligned USPS and MNIST digits in the latent space. (a) Transformed USPS digits look like MNIST digits visually. (b) According to the distribution of log-odds of the classifiers trained to discriminate USPS from MNIST (left) and transformed USPS from MNIST (right), LRMF learned a transformation of latent codes that made transformed USPS and MNIST indistinguishable by a CNN discriminator. (c) The LRMF objective attains zero upon convergence (red line). Intermediate steps and more examples of transformed USPS digits are given in the supplementary (Figure 10).



loss value in the second experiment dropped below zero (red line) around optima because of the randomness and the size of the minibatch, the expectation of the loss is always positive. This experiment shows that even though the normal family of distributions is not sufficient to approximate moon distributions, it still aligns them *while preserving their local structure*.

**Real NVP and FFJORD LRMF.** For Real NVP experiments we stacked four NVP blocks (spaced by permutations), each block parameterized by a dense neural network for predicting shift and scale with two 512-neuron hidden layers with ReLUs (the “default” Real NVP). We used the Adam optimizer with learning rate  $10^{-4}$  for training. The first line (i) in Figure 5 shows that even with a severely overparameterized  $T$  and  $\mathcal{M}$ , the LRMF model successfully found a meaningful correspondence between two blob datasets, the loss converged to zero, and the density  $\theta_S$  at optima agreed with the density  $\theta_B$ , as expected. The second line (ii) shows that the Real NVP LRMF learned the structure of data manifolds and preserved it during translation. The FFJORD LRMF also converged to zero and performed marginally better than the Real NVP model, the visualizations can be found in the supplementary (Figure 9).

**SN-GAN.** The Spectral Normalization (Miyato et al., 2018) of weights of the the discriminator prevented the adversarial training from collapsing. Unfortunately, as presented in Figure 6, neither the convergence (c,d; blue line) nor the performance (b) of the learned transformation can not be inferred from the objective value alone, and the model tends to diverge from the aligned configuration over time (b). As a result, the overall procedure still requires either visual inspection of transformed samples or an external and domain-specific stopping heuristics, such as the Inception Score or the Frechet Inception Distance. The convergence of the proposed log-likelihood ratio minimizing flow (orange line), on the other hand, can be judged by examining the average objective value alone - if the objective reaches zero, datasets are guaranteed to be aligned with respect to the specified density family.

**Local structure.** Results presented in Figure 7 show that, despite the perfect marginal alignment produced by the EMD and the back-to-back flow composition, among minimization objectives, only LRMF correctly preserved the local structure of the transformed dataset  $A$  (red). The middle row shows where did the points of the “red” domain move after the transformation. Numbers at the bottom of the Figure 6 were obtained by training a 1-nearest neighbor classifier on ground truth labels for  $B$  and testing it on ground truth labels for  $T(A)$ . Results for MMD and EMD are deterministic, so no error bars are provided,  $F \circ G^{-1}$  and LRMF experiments were repeated ten times. The bandwidth of the Gaussian kernel in MMD was chosen to maximize

the classification accuracy. The best alignment produced by the SN-GAN was comparable to the LRMF alignment, but required manual visual assessment for early stopping, as mentioned above.

**USPS-to-MNIST.** We trained a VAE-GAN to embed the combined unlabeled dataset containing digit images from both USPS and MNIST into a shared 32-dimensional latent space. We then trained a Real NVP log-likelihood ratio minimizing flow  $T$  to map latent codes of USPS digits to latent codes of MNIST. Figure 8 shows that LRMF objective attained zero upon convergence and semantically aligned images from two domains. Two bar charts in the middle of Figure 8 show log-odds of the convolutional classifier pre-trained to discriminate original MNIST images from original USPS images (on the left) and log-odds of another classifier (on the right) re-trained to discriminate original MNIST images from *transformed* USPS images at each iteration. Both classifiers were able to perfectly discriminate MNIST from USPS at first (top line) and were unable to discriminate the original MNIST from the *transformed* USPS. More detailed version of this figure with translation results and log-odds at intermediate steps are given in the supplementary (Figure 10)

## 5. Conclusion

In this paper we propose a new dataset alignment objective parameterized by a deep density model and a normalizing flow that, when converges to zero, guarantees that the density model fitted to the transformed source dataset will be optimal for the target, and vice versa. We also show that it is robust to model misspecification and preserves local structure of the dataset better than other non-adversarial alignment objectives and a composition of inverted normalizing flows.

## 6. Acknowledgements

This work was partially supported by NSF award #1724237 and DARPA.

## References

- Arjovsky, M., Bottou, L., Gulrajani, I., and Lopez-Paz, D. Invariant risk minimization. *arXiv preprint arXiv:1907.02893*, 2019.
- Bradbury, J., Frostig, R., Hawkins, P., Johnson, M. J., Leary, C., Maclaurin, D., and Wanderman-Milne, S. JAX: composable transformations of Python+NumPy programs, 2018. URL <http://github.com/google/jax>.
- Dillon, J. V., Langmore, I., Tran, D., Brevdo, E., Vasudevan, S., Moore, D., Patton, B., Alemi, A., Hoffman, M. D., and Saurous, R. A. Tensorflow distributions. *CoRR*, abs/1711.10604, 2017. URL <http://arxiv.org/abs/1711.10604>.
- Dinh, L., Sohl-Dickstein, J., and Bengio, S. Density estimation using real nvp. *arXiv preprint arXiv:1605.08803*, 2016.
- Ganin, Y., Ustinova, E., Ajakan, H., Germain, P., Larochelle, H., Laviolette, F., Marchand, M., and Lempitsky, V. Domain-adversarial training of neural networks. *The Journal of Machine Learning Research*, 17(1):2096–2030, 2016.
- Grathwohl, W., Chen, R. T., Bettencourt, J., Sutskever, I., and Duvenaud, D. Ffjord: Free-form continuous dynamics for scalable reversible generative models. *arXiv preprint arXiv:1810.01367*, 2018.
- Grover, A., Chute, C., Shu, R., Cao, Z., and Ermon, S. Alignflow: Learning from multiple domains via normalizing flows. In *2019 Deep Generative Models for Highly Structured Data, DGS@ ICLR 2019 Workshop*, 2019.
- Kingma, D. P. and Dhariwal, P. Glow: Generative flow with invertible 1x1 convolutions. In *Advances in Neural Information Processing Systems*, pp. 10215–10224, 2018.
- Long, M., Cao, Y., Wang, J., and Jordan, M. I. Learning transferable features with deep adaptation networks. *arXiv preprint arXiv:1502.02791*, 2015.
- Long, M., Zhu, H., Wang, J., and Jordan, M. I. Deep transfer learning with joint adaptation networks. In *Proceedings of the 34th International Conference on Machine Learning-Volume 70*, pp. 2208–2217. JMLR. org, 2017.
- Miyato, T., Kataoka, T., Koyama, M., and Yoshida, Y. Spectral normalization for generative adversarial networks. In *International Conference on Learning Representations*, 2018. URL <https://openreview.net/forum?id=B1QRgziT->.
- Nalisnick, E., Matsukawa, A., Teh, Y. W., Gorur, D., and Lakshminarayanan, B. Do deep generative models know what they don’t know? *arXiv preprint arXiv:1810.09136*, 2018.
- Ren, J., Liu, P. J., Fertig, E., Snoek, J., Poplin, R., Deprieto, M., Dillon, J., and Lakshminarayanan, B. Likelihood ratios for out-of-distribution detection. In *Advances in Neural Information Processing Systems 32*, pp. 14680–14691. Curran Associates, Inc., 2019.
- Rezende, D. J. and Mohamed, S. Variational inference with normalizing flows. *arXiv preprint arXiv:1505.05770*, 2015.
- Sun, B. and Saenko, K. Deep coral: Correlation alignment for deep domain adaptation. In *European conference on computer vision*, pp. 443–450. Springer, 2016.
- Tzeng, E., Hoffman, J., Saenko, K., and Darrell, T. Adversarial discriminative domain adaptation. In *Proceedings of the IEEE Conference on Computer Vision and Pattern Recognition*, pp. 7167–7176, 2017.
- van der Ouderaa, T. F. and Worrall, D. E. Reversible gans for memory-efficient image-to-image translation. In *Proceedings of the IEEE Conference on Computer Vision and Pattern Recognition*, pp. 4720–4728, 2019.
- Yang, G., Huang, X., Hao, Z., Liu, M.-Y., Belongie, S., and Hariharan, B. Pointflow: 3d point cloud generation with continuous normalizing flows. In *Proceedings of the IEEE International Conference on Computer Vision*, pp. 4541–4550, 2019.

## 7. Supplementary Material

### 7.1. Pseudo-code for the learning algorithm

This pseudo-code generally follows the JAX implementation we provide, the actual LRMF is trained in mini-batches.

```
def build_lrnf(A, B, L, flow, minimize):
    """ Returns the LRMF objective.

    A, B: datasets
    L: (dataset, theta) -> float
        returns the mean negative
        log-likelihood of the dataset given
        params theta of the model from M
    flow: (flow_L, flow_prior, flow_apply)
    flow_L: (dataset, phi) -> float
        flow negative log-likelihood
    flow_prior: dataset -> float
    flow_apply: (dataset, phi) -> dataset
    minimize: ((param) -> float) -> param
        returns the argument that minimizes
        the given function wrt param
    """
    flow_L, flow_prior, flow_apply = flow
    theta_a = minimize(lambda th: L(A, th))
    theta_b = minimize(lambda th: L(B, th))
    ent_a = L(A, theta_a)
    ent_b = L(B, theta_b)
    prior_a = flow_prior(A)
    const = prior_a + ent_a + ent_b
    def lrnf_objective(theta_s, flow_phi):
        a_t = flow_apply(A, flow_phi)
        ent_at_s = L(a_t, theta_s)
        ent_b_s = L(B, theta_s)
        ent_phi = flow_L(a_t, flow_phi)
        loss = ent_at_s + ent_b_s - ent_phi
        return loss - const
    return lrnf_objective

def train_lrnf(*params):
    """ Returns optimal LRMF parameters.

    Same arguments as in 'build_lrnf'.
    """
    lrnf_loss = build_lrnf(params)
    _, best_phi = minimize(lrnf_loss)
    return best_phi
```

### 7.2. Attached code

Attached IPython notebooks were tested to work as expected in Colab. The JAX version includes experiments on 1D and 2D Gaussians and Real NVP, the Tensorflow Probability (TFP) version includes experiments on Real NVP and FJORD.

### 7.3. Dataset parameters

Blobs datasets were samples from 2-dimensional Gaussians with parameters

$$\mu_A = \begin{bmatrix} 1.0 \\ 1.0 \end{bmatrix}, \Sigma_A^{-\frac{1}{2}} = \begin{bmatrix} 0.5 & 0.7 \\ -0.5 & 0.3 \end{bmatrix}$$

$$\mu_B = \begin{bmatrix} 4.0 \\ -2.0 \end{bmatrix}, \Sigma_B^{-\frac{1}{2}} = \begin{bmatrix} 0.5 & 3.0 \\ 3.0 & -2.0 \end{bmatrix}.$$

Moons dataset pairs were generated with  $\varepsilon = 0.05$  containing 2000 samples each.

### 7.4. On the relation to the Invariant Risk Minimization

In a recent arXiv submission, Arjovsky et al. (2019) suggested that in the presence of an observable variability in the environment  $e$  (e.g. labeled night-vs-day variability in images) the representation function  $\Phi(x)$  that minimizes the conventional empirical risk across all variations actually yields a subpar classifier. One interpretation of this statement is that instead of searching for a representation function  $\Phi(x)$  that minimizes the expected value of the risk

$$\mathcal{R}^e(f) = \mathbb{E}_{(X,Y) \sim P_e} l(f(X), Y)$$

across all variations in the environment  $e$ :

$$\min_{\Phi} \min_{\theta} \mathbb{E}_e \mathcal{R}^e(f(\Phi(\cdot), \theta))$$

one should look for a representation that is optimal under each individual variation of the environment

$$\min_{\Phi} \left[ \min_{\theta} \mathbb{E}_e \mathcal{R}^e(f(\Phi(\cdot), \theta)) - \mathbb{E}_e \min_{\theta_e} \mathcal{R}^e(f(\Phi(\cdot), \theta_e)) \right]$$

Authors linearise this objective combined with the conventional ERM around the optimal  $\theta$ , and express the aforementioned optimality across all environments as a gradient penalty term that equals zero only if  $\Phi$  is indeed optimal across all environment variations:

$$\min_{\Phi} \min_{\theta'} \mathbb{E}_e \mathcal{R}^e(f(\Phi(\cdot), \theta')) + \lambda \mathbb{E}_e \|\nabla_{\theta} \mathcal{R}^e(f(\Phi(\cdot), \theta'))\|_2.$$

This procedure and the resulting objective are very much reminiscent of the log-likelihood ratio minimizing flow objective we propose in this paper, and the score test version we would have obtained if we linearized our objective around the optimal  $\theta_S$ . The main difference being that Arjovsky et al. (2019) applied the idea of invariance across changing environments to the setting of supervised training via risk minimization, whereas we apply it to unsupervised alignment via likelihood maximization.



### 7.5. FFJORD LRMF on moons.

As mentioned in the main paper, FFJORD LRMF performed on par with Real NVP version. We had to fit  $T(x, \phi)$  to identity function prior to optimizing the LRMF objective, because the glorot uniform initialized 5-layer neural network with tanh non-linearities (used as a velocity field in FFJORD) generated significantly non-zero outputs. The dynamics can be found in the Figure 7.

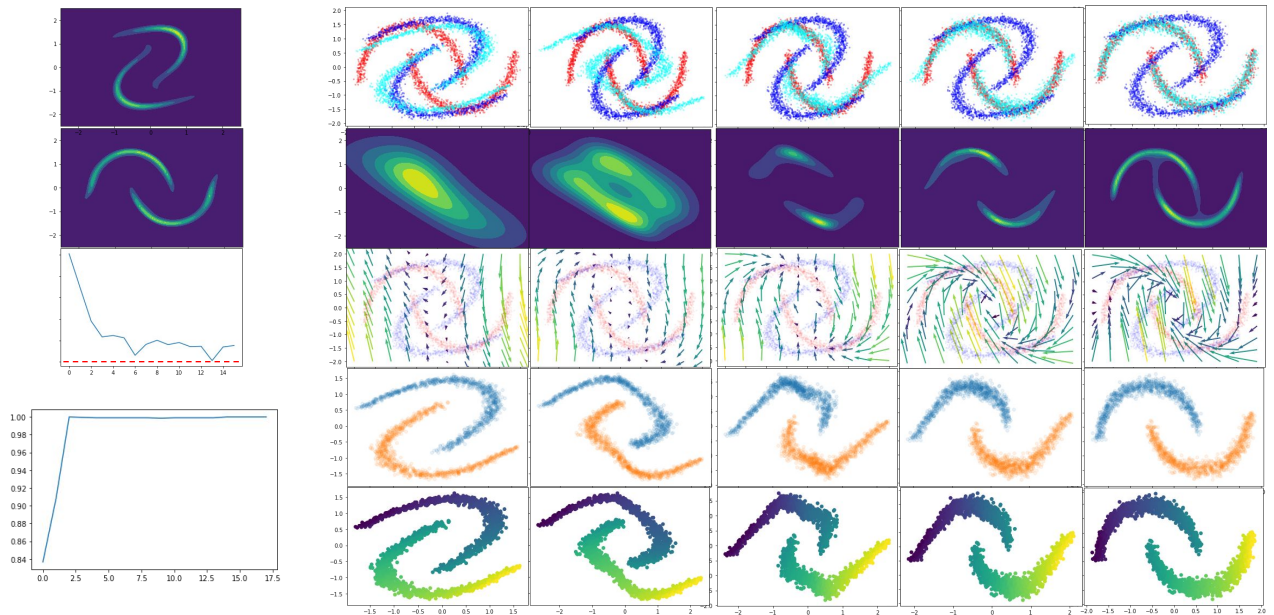


Figure 9. The dynamics of training a FFJORD log-likelihood ratio minimizing flow (LRMF) on the moons dataset. Notations are similar to Figures 5 and 6. The left bottom plot shows changes in accuracy over time.

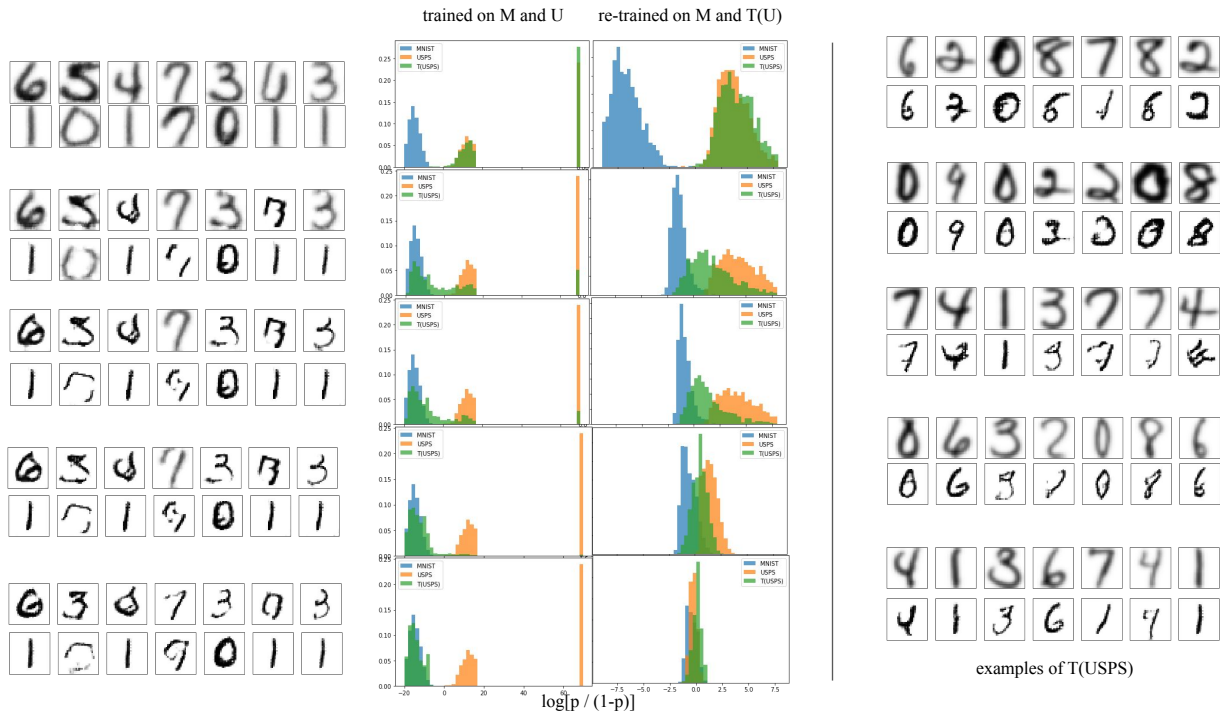


Figure 10. The dynamics of RealNVP LRMF semantically aligning USPS and MNIST digits in the latent space. Notations are similar to Figures 8. Different rows on the left represent different time steps. The right side of the figure shows more examples of transformed USPS digits.